Composites Science and Technology **23** (1985) 263–285

Corrosion Phenomena in Glass Fibers and Glass Fiber Reinforced Thermosetting Resins*

A. Bledzki,† R. Spaude‡ and G. W. Ehrenstein

Department of Materials Technology, University of Kassel,
Wilhelmshöher Allee 73, D-3500 Kassel (FRG)

SUMMARY

Specific interactions between chemical environments and glass fibers cause stress corrosion cracking in the glass fiber surface. The interaction between fibers and diluted acids can be characterized readily in terms of a visible core/shell morphology that develops during the extraction process. The investigations revealed several correlations between the extraction process, crack formation phenomena and fiber strength.

The corrosive environments clearly have an adverse effect on the fatigue properties of glass fiber reinforced resins. Superimposed on mechanically induced damage is a chemical damage component, which becomes increasingly important at longer testing times and hence at lower stress levels. Since corrosive environments act primarily to reduce the fiber strength, their influence is controlled by diffusion processes through the matrix and by penetration of the chemically aggressive substance into the material interior through cracks. While the latter mechanism is especially important for fatigue loading conditions, it can be assumed that the degree of damage will generally depend upon several factors such as glass content, test temperature, and the aggressiveness of the chemical environment.

* Paper presented at the International Symposium, 'Composites: Materials and Engineering', University of Delaware, Newark, Delaware, USA, September 24–28, 1984.
† On leave from the Institute of Chemical Technology, University of Szczecin, Poland.
‡ Currently at BBC AG, Baden, Switzerland.

1 INTRODUCTION

One of the functions of a polymeric matrix in a fiber composite is to protect the fibers from chemical attack through corrosive environments. However, since corrosive liquids (or vapors) may diffuse through the matrix material,[1-4] corrosion effects on fibers may lead to substantial reductions in mechanical properties (i.e. tensile strength, modulus, strain to break), and in some cases may even induce component failure. Well-known examples are failures of storage containers for diluted sulfuric acid,[5] and failures of pipes and containers for solutions of sodium hypochlorite, caustic soda and hydrochloric acid.[6] Similar problems may also occur in waste pipes under high pressure where certain bacteria produce diluted sulfuric acid. It is now generally accepted that glass fiber reinforced (gfr) materials and structures can be severely weakened through the influence of many electrolytes (diluted acid, base and salt solutions).

The purpose of this report is to describe corrosion processes in glass fibers and gfr composites in more detail. In addition, effects of the chemical environment on crack formation phenomena, single fiber strength and on the fatigue resistance of laminates are discussed.

2 CORROSION OF SINGLE GLASS FIBERS

2.1 Microscopic investigation of the extraction process

The fact that even water may corrode glass fibers has been known for many years.[7] In this context it has been suggested that water dissolves alkali ions from the glass surface and thus reduces the effective cross-sectional area of the remaining silicic acid substructure.[8] Furthermore, it has been argued previously[9,10] that there is a fundamental difference between the interaction mechanisms of acids and glass, and those of bases and glass. For example, acids predominantly act to 'leach' or 'extract' glass, i.e. the cations of glass are replaced by H^+-ions of the acidic environment. The layer of silicic acid that remains on the glass surface initially reduces, and finally nearly terminates any further cation exchange. The etching effect of bases, on the other hand, is to remove entire layers from the glass surface in a rather uniform way.

Apparent lumen formation, i.e. the development of the fiber core and

fiber shell, originally described by Bobeth and Schöne,[11] was also observed in E-glass fibers that had been treated with sulfuric acid.[12] The mechanisms involved were investigated in a subsequent study in more detail.[13] This apparent lumen formation occurs in E-glass fibers after exposure to sulfuric and hydrochloric acid of various concentrations and over a range of temperatures. The thickness of the surface region (fiber skin or shell), which is first visible as a thin layer of selectively extracted material, increases with increasing extraction time. The development of such a core/shell morphology was also observed by Metcalfe *et al.*[14] when exposing E-glass to diluted hydrochloric acid.

Extraction experiments on single glass fibers

Five or six glass fibers were mounted in a special container filled with a diluted acid solution and were observed by means of an optical microscope equipped with a hot plate. The arrangement was such that all the fibers could be photographed (Fig. 1), and the dimenions of interest

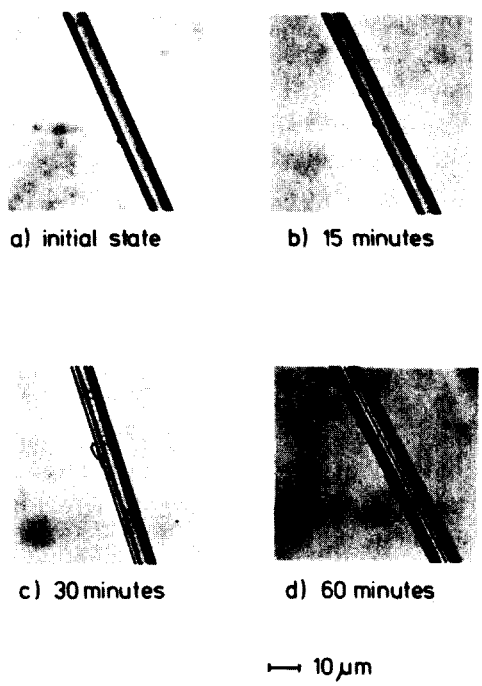

Fig. 1. An E-glass fiber at various stages of the leaching process in 1 % sulfuric acid at 80 °C.

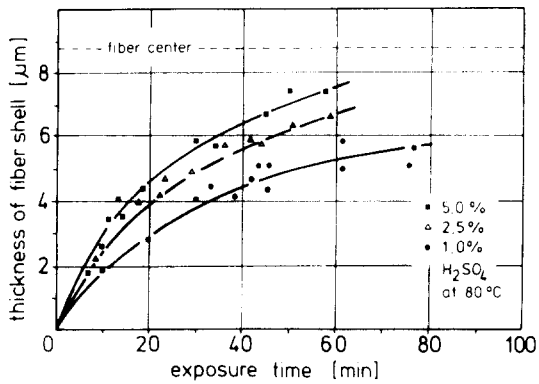

Fig. 2. Thickness of the fiber-shell in E-glass fibers as a function of exposure time to sulfuric acid of various concentrations.

could be measured. The temperature was held constant at 80 °C in order to decrease the time scale for the extraction experiments.

To describe the progress of the extraction process, the thickness of the leached fiber surface layer (fiber shell) was taken as a measure. The dependence of surface layer thickness on extraction time is illustrated in Fig. 2 for three different concentrations of sulfuric acid. While fibers are leached more or less completely, depending on the initial fiber diameter and other experimental conditions, an increase in acid concentration clearly accelerates the extraction process. According to another study,[15] high and very low concentrations are less dangerous.

Several of the experiments were interrupted following a predetermined time schedule in order to obtain fibers with various core diameters. These fibers were then rinsed carefully with distilled water and were subsequently stored in a water bath for several days. Although the core/shell morphology was still clearly visible, no grooves or cracks developed, nor could any other changes be observed.

Separate experiments were conducted to investigate whether the application of a size coating has any effect on the extraction process. However, no significant differences could be detected when using solutions of 1 % to 5 % HCl and H_2SO_4 (Fig. 3). Hence, a size coating by itself does not protect glass fibers against corrosive environments. This finding seems reasonable considering that commercially available E-glass fibers are believed to be covered only to the extent of about 50 % with size coatings or coupling agents.[16]

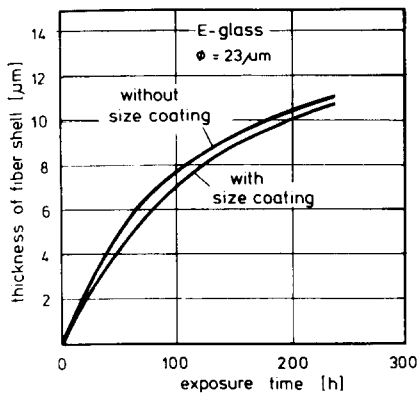

Fig. 3. Effect of the size coating on the leaching process.

Mineral acids that diffuse to the fiber/matrix interface react with the siloxane coupling agent and the outer layer of the glass fiber, and as a result the strength of the fibers decreases. Even if glass fibers are extracted to only a limited extent and subsequently treated with a siloxane coupling agent, values for the composite strength do not improve despite the anticipated improvement in the interfacial strength.

Another factor should be kept in mind when considering leaching of fibers in polymer matrix composites. Owing to the relatively low acid concentration in composites (which is controlled by diffusion processes through the resin) and the simultaneously diminishing supply of H^+-ions, the extraction process may be converted into a basic reaction. The latter may lead to the breaking of siloxane groups and to the formation of Si–O–Na groups, as well as to the partial dissolution of the glass surface.

Micro-mechanisms of the extraction process

Some experiments have revealed that fibers generally leach faster at the fiber surface than in the fiber center. Moreover, the extraction velocity has been found to depend on winding speed during filament production. These effects, together with the behavior illustrated in Fig. 2, cannot be related to local changes in the chemical composition of a glass fiber from the fiber surface to the fiber core. Their cause is apparently more likely to be related to the specific conditions of filament production. Of particular importance is the fact that the temperature distribution which develops across a fiber during the fabrication process (with lowest and highest temperatures, respectively, at the fiber surface and in the fiber center)

leads to higher values of viscosity at the fiber surface. Furthermore, transformations associated with shear and strain flow effects increase the local viscosity at the fiber surface even further. The radial variations in viscosity, together with the winding forces, induce radial variations in melt flow velocities, which in turn imply a shear stress distribution. As a result of the maximum in the temperature gradient, and consequently also in the viscosity gradient, the highest shear stresses develop where the glass exudes from the holes of the bushings, so that the glass fiber loses its isotropic character. 'Multiple layers' develop which glide against each other (Fig. 4) and bonds are broken along the 'gliding planes'. Since such 'gliding planes' are generated to a greater extent in the outer layers of the fibers, the molecular structure becomes more open towards the fiber surface.[16] Furthermore it has been argued that an orientation of Si–O rings may occur in the drawing direction, a factor which would facilitate ion flow in radial directions.[17]

The assumptions that Si–O groups are being stretched during the melt spinning process and that chains, which become oriented along the fiber axis during processing, exist in the glass melt, have also been made by other authors.[12] For example, Wiedemann[12,18] suggested that the structure of glass fibers is more open than that of bulk glass (i.e. glass fibers consist of a more strained SiO_2-network with a lower packing density). In addition, the contraction in fiber length and the simultaneous increase in fiber diameter ($+ \sim 10\%$) caused by the acid treatment can be rationalized in terms of a small structural expansion.[18,24]

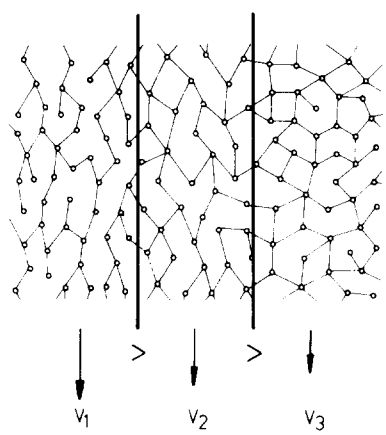

Fig. 4. Schematic illustration of the glass fiber substructure which is induced by the velocity profile across the fiber during processing.

When comparing fibers drawn at speeds of $66{\cdot}7\,m\,s^{-1}$ and $21{\cdot}6\,m\,s^{-1}$, it is important to note that the effects just described occur to a stronger extent in the former case. Hence, not surprisingly, the extraction process was found to be faster for fibers drawn at $66{\cdot}7\,m\,s^{-1}$. This implies also that the study of extraction processes may provide some insight into existing internal stresses in glass fibers. Moreover, experiments of this kind (i.e. using an optical microscope) can be applied to obtain a relative measure of the corrosion resistance of E-glass fibers exposed to diluted acids.

2.2 Crack development

Since no cracks were visible in the acid-treated glass fibers in the wet condition (neither in free fibers nor in fibers in the laminate), the water was evaporated while the fibers were observed continuously in an optical microscope. After complete evaporation of water, crack formation was indeed observed. Since the drying process is associated with relaxation of internal stresses, the entire glass fiber started to move. Depending on the experimental conditions (i.e. acid concentration, extraction time and temperature) various crack shapes and configurations developed at least over part of the fiber length. These included radial and axial cracks, and spiral cracks with various pitch angles.

At first an attempt was made to find a correlation between the observed crack shapes and the time fibers had been exposed to the acidic solution. Figure 5 reveals that the relative contribution of glass fibers that formed 'spiral cracks' initially increases with exposure time and reaches a maximum (of approximately 40 %) at approx. 45 h. This time period

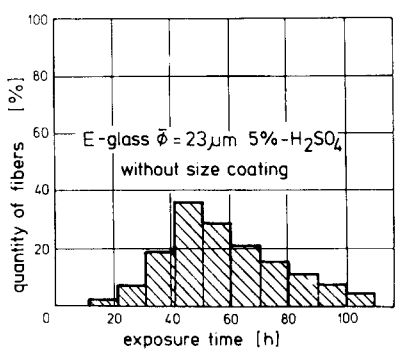

Fig. 5. Histogram of frequency of spiral crack formation in E-glass fibers.

corresponds to a penetration depth of about $\frac{1}{3}$ of the fiber diameter. For smaller values of the penetration depth the number of spiral cracks and radial cracks decreases rapidly so that fibers remain to a large extent intact. In sharp contrast, axial cracks develop only in highly leached glass fibers (core diameter $< \frac{1}{3}$ fiber diameter). In fact, the propensity to form axial cracks is maximized for entirely leached glass fibers, i.e. fibers that had been exposed to the acidic environment for long times.

There was no apparent correlation between the pitch angle of spiral cracks and the thickness of the extracted outer layer of a fiber. It should be mentioned, however, that spiral cracks have also been encountered in fiber reinforced composites (Fig. 6). While the formation and development of spiral cracks occurs roughly at crack speeds of the order of 10^{-6} to $10^{-4}\,m\,s^{-1}$, according to observations in the microscope, a more accurate measure for crack velocities may be obtained by means of cinematographic techniques.[19] Nevertheless, the values cited above are in good agreement with those reported elsewhere for other types of glass.[20]

In some instances cracks were found to propagate without interruption along fibers over the entire field of view; in others they were seen to be terminated at previously developed radial cracks. Occasionally, however, cracks that started out as spiral cracks developed into radial cracks. For such cracks the propagation direction changed from some angle (pitch

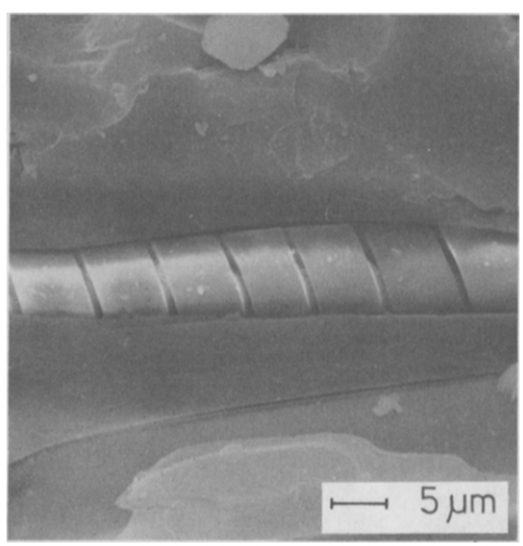

Fig. 6. Spiral crack formation in an E-glass fiber embedded in the polymeric matrix.

angle $>0°$) to a direction perpendicular to the fiber axis (pitch angle $= 0°$),[1] thus providing a mechanism that led to self-termination of spiral crack propagation. In addition, it was frequently observed that crack advance is not a continuous process but rather takes place in interrupted sequences (e.g. fast crack propagation around the fiber perimeter for one turn—no crack growth for a few seconds—fast crack propagation, etc.). Of course, each of these steps causes the fiber to move somewhat, a process which was clearly visible in the microscope. Other workers have shown evidence of somewhat different crack features, both in single glass fibres and in grp materials exposed to corrosive treatments.[21]

It should be emphasized that spiral cracks develop only in fiber surface layers which have undergone substantial changes due to the extraction process. The acidic environment not only acts to dissolve alkali and alkaline earth metals, but also extracts aluminum and boron. This implies that the entire network structure is being broken at certain locations and thus relaxes. The subsequent process of drying the leached layers leads to crack formation and growth. Owing to the evaporation of water molecules (which follows the earlier exchange of metal ions against the much smaller hydrogen protons), contraction forces develop in both axial and circumferential (hoop) directions of the fiber. Based on the observation of the rather small pitch angles in spiral cracks it is concluded that the forces in the axial direction must be significantly larger than those in the hoop direction. In this context it has also been suggested that the formation of spiral cracks is related to the dissolution of B_2O_3.[13] For high values of penetration depth the hoop forces become sufficiently large and axial cracks develop.

2.3 Analysis of extracted elements

Application of X-ray microanalysis has shown[22] that 5% sulfuric acid not only dissolves alkali ions from E-glass but also extracts calcium, magnesium and aluminum (Fig. 7). Further investigations revealed that boron is also leached out.[22] Hence, depending on the extraction conditions, different amounts of these elements can be detected in the leached shell of a fiber (Table 1) although no differences can be observed in the optical microscope. In other words, the composition and structure of the leached surface layers of fibers may well vary (i.e. the amount of dissolved ions and number of broken bonds in the network caused by the

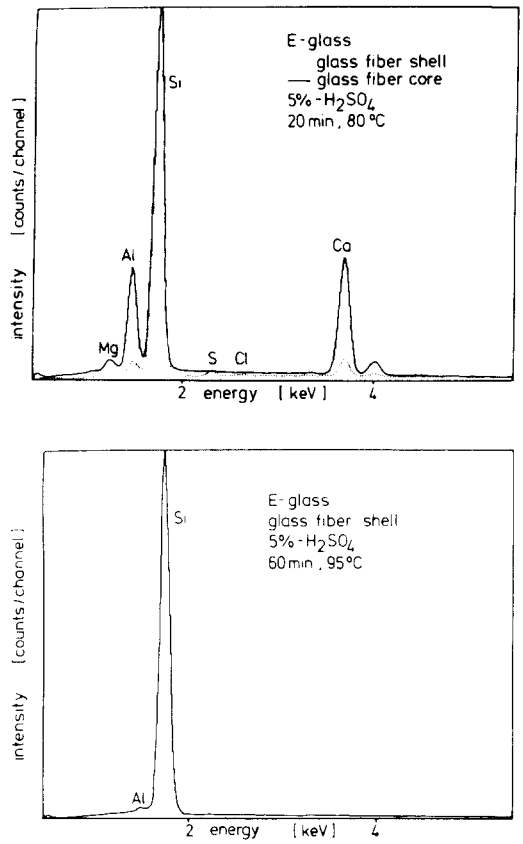

Fig. 7. X-ray spectra of E-glass fibers.

dissolution of boron and aluminium), despite the fact that no differences can be detected optically. Such structural and compositional variations in the leached fiber surface layer depend not only on the experimental conditions of extraction, but also on the fiber processing conditions.

2.4 Strength considerations

Along with the extraction experiments, data were generated on some characteristic mechanical properties. By contrast with previous investigations, the values presented below for fiber tensile strength and Young's modulus were computed on the basis of the remaining cross-section of the corresponding fiber core, since the leached surface layers

TABLE 1
Composition of E-glass Fibers After Exposure to 5% Sulfuric Acid
(Element content given relative to the content of silicon, E/Si)

Relative element content E/Si	*Fiber core*	*Fiber shell*	
		20 min 80 °C	*60 min 95 °C*
Mg/Si	0·036	0·005	0·002
Al/Si	0·267	0·041	0·011
Ca/Si	0·414	0·088	0·005

hardly contribute to the overall fiber strength (only very little force is necessary to remove the surface layer). While there is a sharp decrease in fiber strength to about $\frac{1}{3}$ of that of the untreated fiber for short extraction times, the fiber strength remains nearly constant or even increases again somewhat at longer times (Fig. 8). Similar tendencies have been found for other extraction temperatures and for glass fibers produced by different

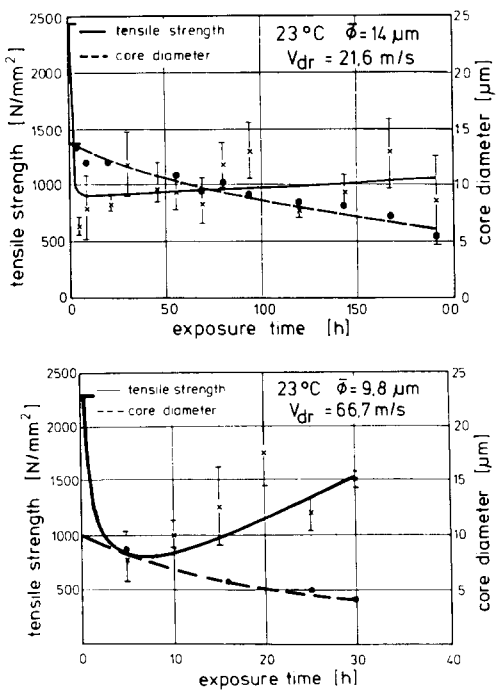

Fig. 8. Tensile strength and fiber core diameter as a function of exposure time for E-glass fibers produced at two different drawing speeds.

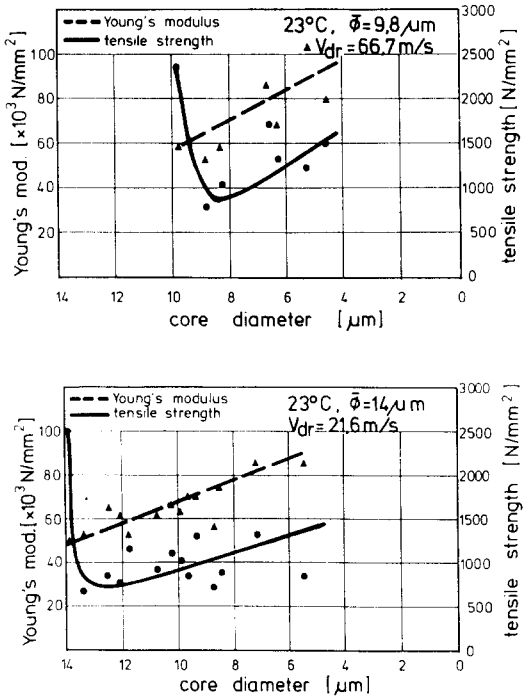

Fig. 9. Tensile strength and Young's modulus as a function of fiber core diameter for E-glass fibers produced at two different drawing speeds.

fabrication conditions. Moreover, values for Young's modulus were found to increase with decreasing core diameter (Fig. 9); the strain to break was of the order of 4% and 1–2%, respectively, for untreated and leached fibers.

The increase in both fiber strength and Young's modulus with decreasing fiber core diameter can be rationalized in terms of the increase in glass density (the slower the cooling rate the higher the density[23]), and the more uniform structure of the fiber core (i.e. stretch effects are less pronounced in this region).

Figure 10 shows that other types of glass fibers are also affected by corrosive environments. While the fiber tensile strength decreases continuously with extraction time in all cases, at least initially, it should be noted that the most significant decrease occurs within the first 100 h. In this case the tensile strength is related to the original cross-section, in contrast to Fig. 8 where the strength is related to the core diameter.

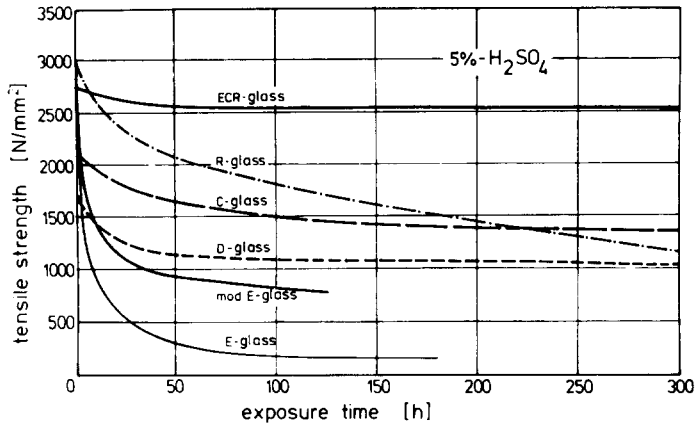

Fig. 10. Tensile strength as a function of exposure time for different types of glass fibers.

3 CORROSION PHENOMENA IN LAMINATES

3.1 Experimental procedure and materials

Two types of fatigue experiments, reversed bending tests and fatigue crack propagation (FCP) tests, were carried out under various environmental conditions such as laboratory air, water, and 1 % and 5 % sulfuric acid. In the bending experiments the decay in stress amplitude, σ_a, under constant deflection range conditions was measured and evaluated in terms of the applied cycle number, N (dynamic stress relaxation behavior). In the FCP experiments, on the other hand, the crack length, a, in compact tension (CT) specimens was measured under constant load range conditions as a function of the cycle number (load ratio $R = F_{min}/F_{max} = 0{\cdot}125$, where F is the applied load). In this case crack growth rates, da/dN, were interpreted in terms of the crack tip stress intensity factor range, ΔK. To reduce or eliminate the tendency for hysteretic heating, loading frequencies ranging from 5 to 7 Hz were used.

The reversed bending experiments were performed on E-glass fiber reinforced laminates of chopped strand mat (27 %wt glass) and on laminates of woven roving fabric (50 %wt glass). In the FCP tests, on the other hand, E- and ECR-glass reinforced mat laminates (34 %wt glass) were used to investigate the influence of the fiber corrosion resistance on the FCP behavior of these materials in various environments.

Unsaturated polyester (UP) resins based on orthophthalic acid and standard glycols dissolved in styrene were used as matrix materials. The UP-resins for the materials tested under reversed bending conditions were of low viscosity and medium reactivity, while those for the FCP experiments were of medium viscosity and high reactivity. Laminates were produced by hand lay-up techniques and cured at 80 °C for 5 h to achieve a high degree of curing (99·9 %). Further details as to the experimental set-up, the data reduction scheme, and the materials are described elsewhere.[24,25]

3.2 Results

Reversed bending tests

The stress amplitude versus cycle number results are plotted in Fig. 11 for mat laminates and woven roving laminates tested in air at various initial stress amplitudes, $\sigma_{a(N=1)}$. Stress decay effects under constant deflection are clearly more pronounced in the former material. Of particular importance, however, is that there is an inflection point in the σ_a-N curves, at least at higher values of $\sigma_{a(N=1)}$. Thus for $\sigma_{a(N=1)}$ between 40 and 60 N mm^{-2} the stress decay rate (i.e. $da/d(\log N)$) first increases, and at higher cycle numbers decreases again somewhat because of stress

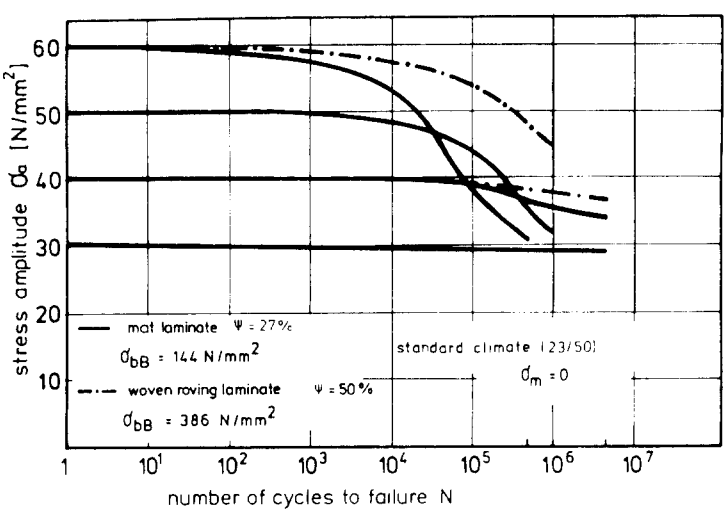

Fig. 11. Dynamic stress relaxation curves for mat and woven roving laminates in air. σ_m = mean strength; σ_{bB} = flexural strength; ψ = glass content (weight %).

relaxation effects associated with crack and damage development at the specimen surface where cyclic stresses are highest. Since the stress decay for $\sigma_{a(N=1)} = 30\,\mathrm{N\,mm^{-2}}$ even after 2×10^6 cycles is only of the order of about 2%, we may expect that for initial stress levels smaller than this both materials will sustain more than 10^7 cycles without a significant stress decrease.

In sharp contrast, Figs 12 and 13 reveal that corrosive environments such as diluted sulfuric acid invariably lead to total stress decay and specimen fracture even at initial stresses as low as $20\,\mathrm{N\,mm^{-2}}$. At low cycle numbers the behavior is similar to that depicted in Fig. 11 for air, and up to about 10^3 cycles hardly any mechanical damage was visible at the specimen surface. With increasing testing time an increasing number of cracks developed. Thus the penetration of sulfuric acid into the glass fibers in the specimen interior, a process which is otherwise controlled entirely by diffusion through the matrix, is facilitated through capillary effects associated with the network of microcracks and interfacial cracks. As a consequence of the enhanced acid/fiber interaction the fiber strength is reduced by stress corrosion cracking, viz., damage resulting from simultaneous mechanical and chemical action, and the fibers lose their reinforcing character. Simultaneously the overall crack formation and propagation rate accelerates owing to stress redistribution effects, and

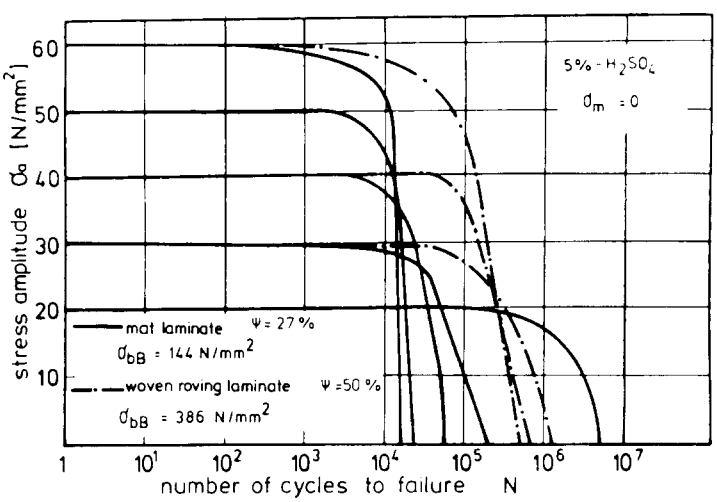

Fig. 12. Dynamic stress relaxation for mat and woven roving laminates in 5% sulfuric acid (symbols as defined for Fig. 11).

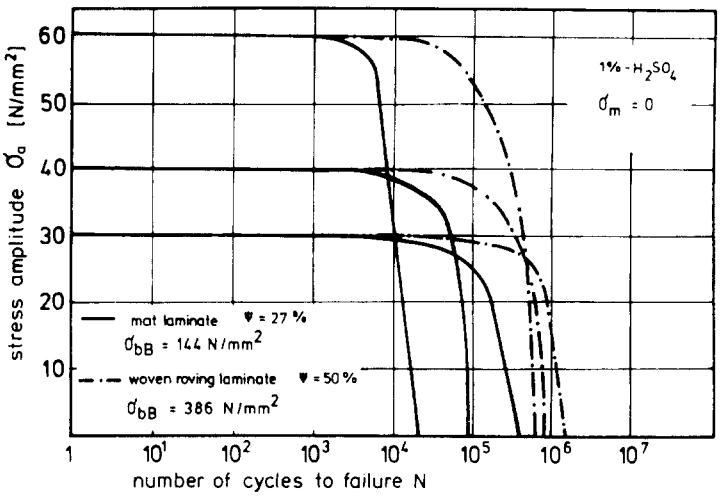

Fig. 13. Dynamic stress relaxation curves for mat and woven roving laminates in 1 % sulfuric acid (symbols as defined for Fig. 11).

ultimate specimen failure occurs within a short time period. The reduction in strength is indicated by the extremely steep, almost vertical, slopes in the dynamic stress relaxation behavior shown in Figs 12 and 13.

Fatigue crack propagation experiments

Unlike that in metals or unreinforced polymers, fatigue crack growth in fiber reinforced plastics does not occur by a smooth and clear-cut mechanism. In general the crack is not a simple entity but consists of a main crack which is surrounded by innumerable side cracks.[26]

The crack propagation behavior of E- and ECR-glass reinforced resins in various environments is compared in Fig. 14(a)–(c) in terms of crack length versus number of cycles. While the cyclic life of the ECR-glass reinforced material is generally higher, the life time in both materials decreases as the chemical aggressiveness of the surrounding environment increases. It should be noted, however, that the relative difference in the number of cycles to failure between the two laminates depends upon the environment. For example, for the given test conditions this relative difference in cyclic lives was found to decrease from a factor of more than 250 in air, to factors of approximately 15 and 10, respectively, in water and 5 % sulfuric acid.

The dependence of crack growth rates, da/dN, on the crack tip stress intensity factor range, ΔK, is shown in Fig. 15(a)–(c). The figures reveal

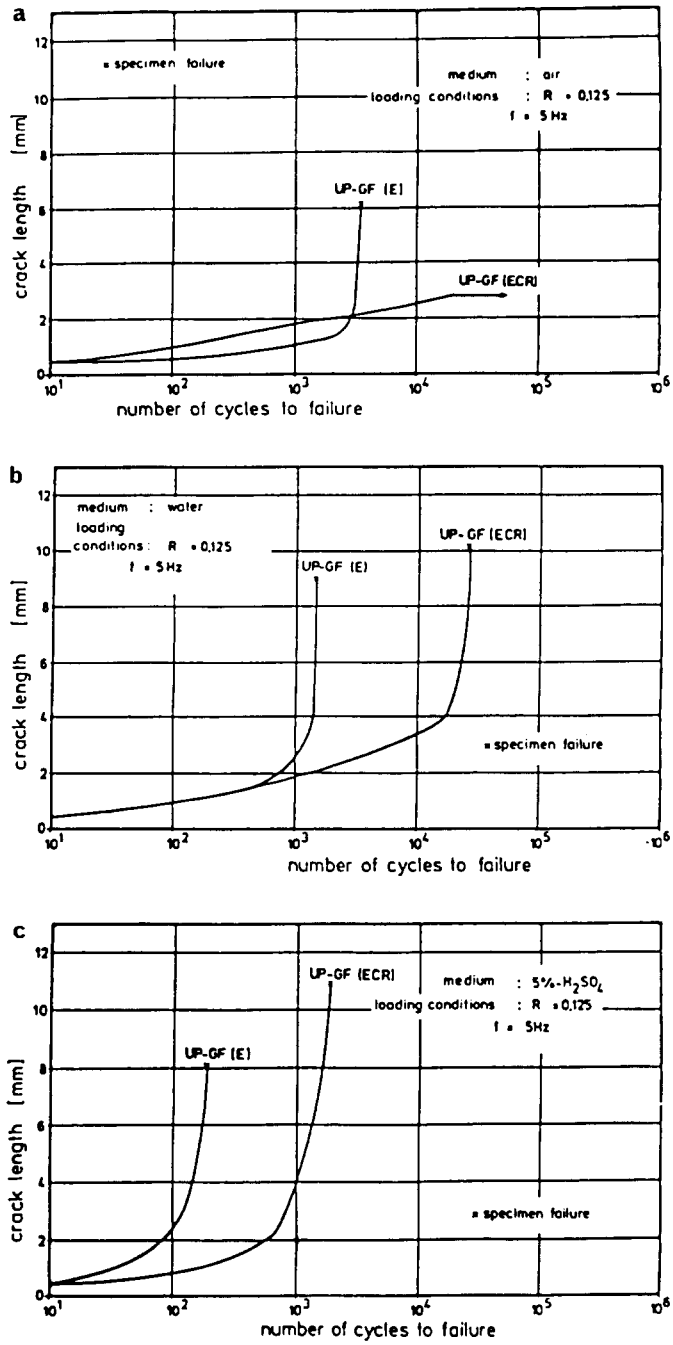

Fig. 14. Crack length vs. number of cycles of E- and ECR-glass fiber reinforced laminates (mean load $F_{mean} = 450\,N$; maximum load $F_{max} = 800\,N$).

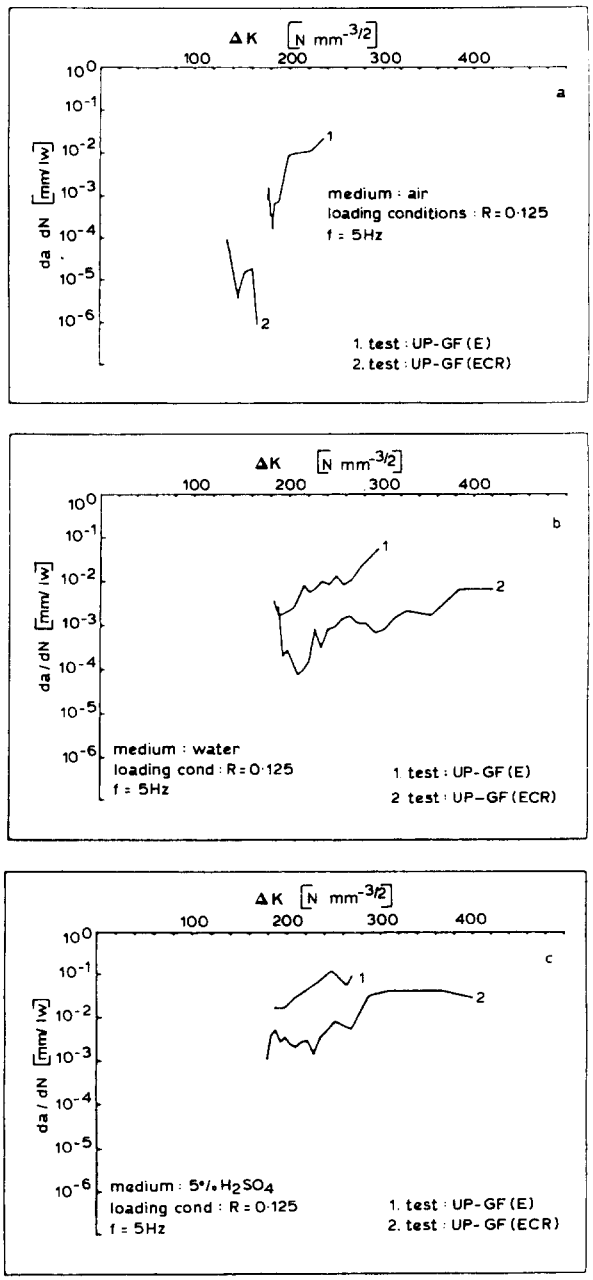

Fig. 15. Fatigue crack propagation behavior of E- and ECR-glass fiber reinforced laminates in various environments. (mm/lw = mm crack extension per cycle.)

that, at a given value of ΔK, crack growth rates in the E-gfr material are about an order of magnitude larger than those in the ECR-gfr material. Moreover, while crack growth rates clearly decrease, at least initially with increasing ΔK in air and water, they increase continuously with ΔK in 5% sulfuric acid. For ΔK levels larger than about 200 N mm$^{-3/2}$, crack growth rates increase with ΔK in all cases up to the point where the maximum stress intensity factor in a loading cycle approaches the fracture toughness of the material and specimen failure takes place.

Fractography

Scanning electron microscopy (SEM) of specimen fracture surfaces of both mat and woven roving laminates tested in 5% sulfuric acid under reversed bending conditions provided some insight into the micro-mechanisms of failure.

Figure 16 was taken from a mat laminate specimen subjected to an initial stress amplitude of 60 MPa. Under these loading conditions total specimen failure occurred after about $1{\cdot}5 \times 10^4$ cycles at 6 Hz, which corresponds to an acid exposure time of about 40 min. Owing to the large stress and deformation amplitudes, high alternating tensile and

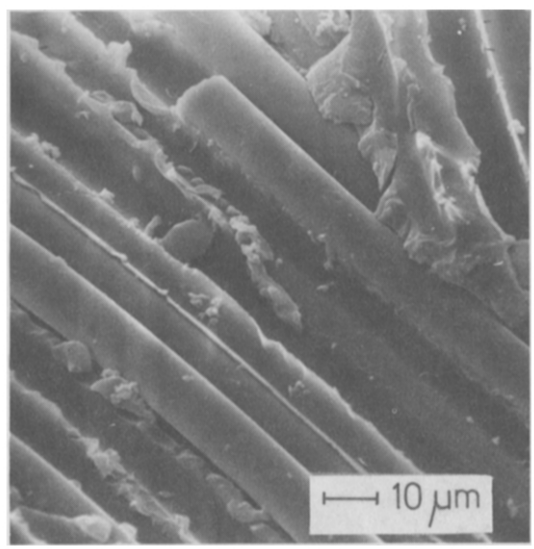

Fig. 16. Scanning electron micrograph from the fracture surface of a mat laminate specimen tested under reversed bending conditions at $\sigma_{a(N=1)} = 60$ MPa (duration of experiment: 40 min; predominantly mechanical failure).

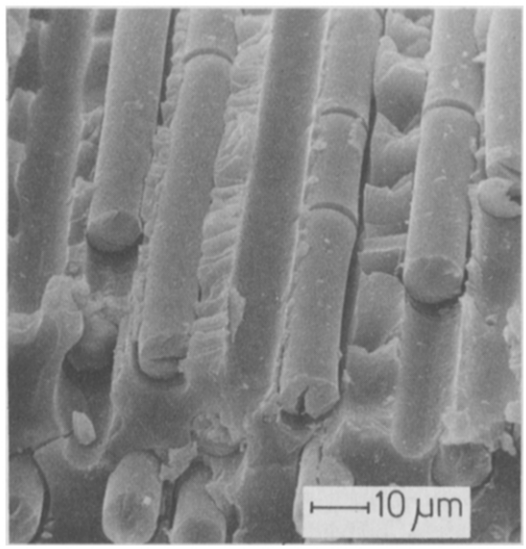

Fig. 17. Scanning electron micrograph from the fracture surface of a mat laminate specimen tested under reversed bending conditions at $\sigma_{a(N=1)} = 40$ MPa (duration of experiment: 13·3 h; mechanical and chemical damage).

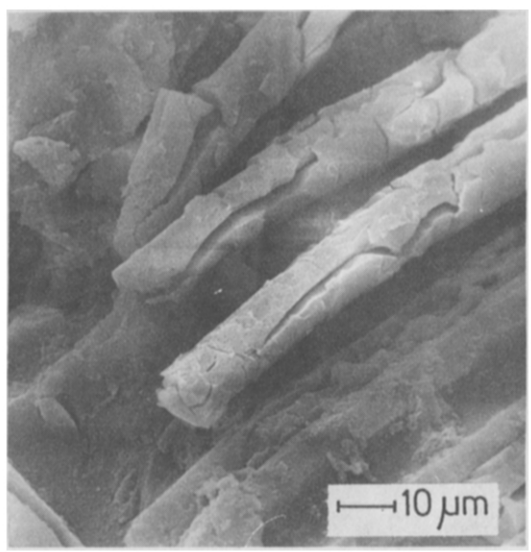

Fig. 18. Scanning electron micrograph from the fracture surface of a mat laminate specimen tested under reverse bending conditions at $\sigma_{a(N=1)} = 20$ MPa (duration of experiment: 164·4 h; predominantly chemical damage).

compressive strains develop at the upper and lower specimen surfaces and these induce substantial shear-stresses locally between fibers and matrix. Nevertheless, although the failure mode is predominantly of a mechanical nature and despite the relatively short exposure to the acidic environment, crack formation indicative of corrosion effects and chemical fiber damage was occasionally visible in the surface layers of some fibers.

While multiple fiber fracture, as shown in Fig. 17, certainly serves as a first indication of the significant effect of sulfuric acid on the fracture behavior of glass fibers in laminates, the degrading influence of the chemical environment is even more apparent in Fig. 18. The long testing time of approx. 164 h that corresponded to the lowest stress level investigated resulted in the longest and consequently most severe chemical attack as is evidenced by fibers broken into many small particles and fragments.

In contrast to the behavior of mat laminates, chemical fiber damage was found to control reversed bending fatigue lives in the woven roving material at all stress levels investigated. This is to a large extent due to the fact that the cyclic lives of the latter material at a given stress level were generally longer; hence the exposure time to acid was also longer (see Fig. 12).

4 SUMMARY AND CONCLUSIONS

Corrosion processes in single E-glass fibers have been studied using optical microscopy and X-ray microanalysis techniques. The great advantage of optical microscopy is that the interaction between fibers and diluted acids can be characterized readily in terms of a visible core/shell morphology that develops during the extraction process. The investigations revealed several correlations between the extraction process, crack formation phenomena and fiber strength.

In addition it has been shown that corrosive environments greatly affect fatigue resistance of E-gfr mat and woven roving laminates. While specimen failure in bending experiments in air was controlled by mechanical degradation and damage accumulation, specimen failure at equivalent initial stress levels in acidic environments occurred at comparatively shorter times as a result of additional adverse effects associated with chemical material degradation. As expected, the influence

of the latter mechanism was found to be the more pronounced the lower the value of the initial cyclic stress amplitude. Although preliminary experiments revealed only a minor influence of a change in acid concentration on the cylic life in these materials, it must be assumed that such effects will generally depend on the specific material-acid combination, and on the applied test conditions.

Fatigue crack propagation experiments on E- and ECR-glass reinforced resins in air revealed a higher FCP resistance in the latter material. The superiority in the behavior of the ECR-glass reinforced material was also found, although to a lesser extent, in experiments in water and sulfuric acid. The FCP resistance of both materials in three different environments was found to decrease in the order: air, water and 5 % sulfuric acid.

In summary, corrosive environments clearly have an adverse effect on the fatigue properties of glass fiber reinforced resins. Superimposed on mechanically induced damage is a chemical damage component which becomes increasingly important at longer testing times and hence at lower stress levels. Since corrosive environments act primarily to reduce the fiber strength, their influence is controlled by diffusion processes through the matrix and by penetration of the chemically aggressive medium into the material interior through cracks. While the latter mechanism is especially important for fatigue loading conditions, it can be assumed that the degree of damage will generally depend upon several factors, such as glass content, test temperature, and the aggressiveness of the chemical environment.

ACKNOWLEDGEMENTS

The authors are grateful to J. Izbicka, Th. Neikes, H.-P. Heitmeier and R. W. Lang for many valuable suggestions and for their help with the experiments.

REFERENCES

1. R. F. Regester, *Corrosion*, **25** (1969), p. 157.
2. B. Alt, *Kunststoffe*, **62** (1972), p. 809.
3. H. Ishida and J. L. Koenig, *Polym. Eng. Sci.*, **18** (1978), p. 128.
4. R. C. Allen, *Polym. Eng. Sci.*, **19** (1979), p. 329.
5. E. Inhoffen, Preprint, 16. AVK-Tagung, Freudenstadt, 1980.

6. B. Alt, *Chemie-Technik*, **4** (1975), p. 237.
7. R. Bennewitz, W. Bobeth and H. Dittmann, *Faserforsch. Textiltech.*, **6** (1955), p. 391.
8. P. A. Koch, in: *Chemische Textilfasern, Filme und Folien* (ed. R. Pummerer), Enke Verlag, Stuttgart, 1953.
9. W. Geffken, *Kolloid-Z.*, **86** (1939), p. 11.
10. H. Schröder, *J. Naturforsch.*, **4** (1949), p. 515.
11. W. Bobeth and A. Schöne, *Faserforsch. Textiltech.*, **17** (1966), p. 214.
12. G. Wiedemann, *Faserforsch. Textiltech.*, **22** (1971), p. 192.
13. G. Wiedemann, W. Bobeth and U. Müller, *Faserforsch. Textiltech.*, **24** (1973), p. 395.
14. A. G. Metcalfe, M. E. Gulden and G. K. Schmitz, *Glass Technology*, **12** (1971), p. 15.
15. S. Torp and R. Arvensen, 34th Annual Conf. Reinforced Plastics Division, SPI, New Orleans, 1979, Section 13-D.
16. U. K. Neumann, Dissertation, University of Erlangen-Nürnberg, 1972.
17. R. Brückner, *Veröffentl. Max-Planck-Institut für Silikatforsch., Würzburg*, **26** (1966), p. 99.
18. G. Wiedemann and H. Frenzel, *Faserforsch. Textiltech.*, **24** (1973), p. 355.
19. G. W. Ehrenstein, A. Bledzki and R. Spaude, *Korrosion von Elementarglasfasern*, Wissenschaftlicher Film, Göttingen, 1983.
20. S. W. Freiman, *Chermurgie Intern.*, **2** (1976), p. 111.
21. F. R. Jones and J. W. Rock, *J. Mat. Sci. Letters*, **2** (1983), p. 415.
22. G. W. Ehrenstein, A. Bledzki, T. Neikes and R. Spaude, *J. Werkstofftech.*, **15** (1984), p. 132.
23. M. J. Oel, M. Dannheim and G. Hellend, *Glastechn. Ber.*, **52** (1979), p. 127.
24. H.-P. Heitmeier, Thesis, Institut für Werkstofftechnik, University of Kassel, 1984.
25. R. Spaude, Dissertation, University of Kassel, 1984.
26. R. W. Lang, J. A. Manson and R. W. Hertzberg, *Advances in Chemistry Series 206*, American Chemical Society, Washington, DC, 1984, p. 261.